MODELING OF SEISMIC WAVE ATTENUATION FOR HELICOPTER DETECTION

Liu Xiaojun, Wang Zhuang

College of Electronic Science and Technology, National University of Defense Technology, Changsha, 410073, China

Annotation. Seismic wave detection technology provides a viable solution for monitoring low-altitude helicopters in border airspace. This paper proposes a seismic wave attenuation model and validates it through numerical simulations.

Keywords. Border defense, low-altitude helicopter, seismic wave detection, seismic wave attenuation

Introduction. Modern aerial vehicles, particularly helicopters, threaten low-altitude border defense. Therefore, developing effective low-altitude helicopter detection technological approaches is essential. The seismic sensor system provides a viable passive detection technology—seismic wave detection—for low-altitude border defense, offering advantages over radar (environmental covertness and anti-electromagnetism interference) and electro-optical systems (non-line-of-sight capability), with additional benefits of low cost, compact size, and flexible deployment. This paper focuses on effectively detect low-altitude helicopters via seismic waves. First, the propagation process from helicopter radiated acoustic waves to seismic wave signals received by sensors is characterized, and a model for Rayleigh wave attenuation is established. Then, the time-domain and frequency-domain models of the received signals are derived. Finally, numerical simulation results and conclusion are presented.

Propagation Process of Helicopter Radiated Acoustic Pressure Signals. Helicopter external noise includes aerodynamic noise (dominant far-field) and mechanical noise (near-field attenuation, negligible). Given the directional radiation pattern of the acoustic field[1], this study focuses on main rotor aerodynamic pressure signals (excluding tail rotor effects). As illustrated in Figure 9, the energy conversion process involves three sequential phases: 1) acoustic propagation in the air, 2) acoustic-seismic coupling at the air-ground interface, and 3) seismic waves propagation to sensors in the ground.

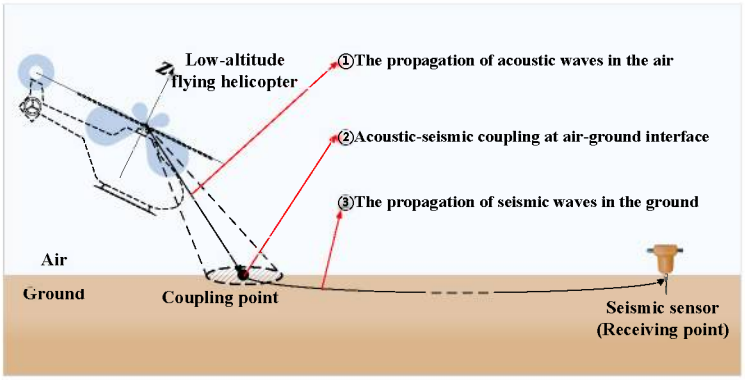

Figure 9 - The propagation process

Seismic Wave Attenuation Model in Propagation Media. Based on Huygens principle, the coupling point can be modeled as new ground vibration source. Previous researches about ground vibration sources have revealed that the energy of Rayleigh waves dominate at long distances (≈67%) due to the much lower attenuation rate. It can be concluded that sensors primarily detect Rayleigh wave energy. Combining absorption and geometric divergence, Rayleigh wave attenuation follows the Bornitz equation:

$$A(r) = A_0 \cdot r^{-0.5} \cdot \exp(-\alpha r) \tag{1}$$

where A_0 is the initial amplitude at the coupling point, $A(r)$ is the amplitude received by sensor at distance r .The term $r^{-0.5}$ refers to the geometric divergence of Rayleigh waves. The parameter α is the absorption attenuation coefficient:

$$\alpha = \frac{\pi f}{V_R Q} \tag{2}$$

where f is the vibration frequency, V_R is the phase velocity of Rayleigh waves, and Q is the quality factor that depends on soil type. However, the in-situ quality factor Q cannot be accurately obtained, restricting the estimation of α using Eq.(2). For this reason, a “frequency-independent” attenuation

coefficient α_0 has been proposed[2], defined as follows:

$$\alpha_0 = \frac{\alpha}{f} = \frac{\pi}{V_R Q} \tag{3}$$

Based on Eq.(3), the coefficient α_0 can be approximated as a constant, making it effectively applicable in estimating absorption attenuation. Consequently, the amplitude attenuation for Rayleigh waves can be further written as given by:

$$A(r) = A_0 \cdot r^{-0.5} \cdot \exp(-\alpha_0 f r) \tag{4}$$

Models of Acoustic Pressure Signal Propagation. *Equivalent Vibration Source Signals at Coupling Point.* The coupling point between the acoustic wave and the ground can be regarded as an acoustic signal receiving point (virtual microphone), then the acoustic pressure signal at the coupling point is given by the following equation (the absolute time delay of acoustic wave propagation from the rotor to the coupling point, being irrelevant to passive detection, is thus omitted for simplicity)[3]:

$$U_{p_L}(t) = \begin{cases} \sum_{j=1}^{J}\sum_{l=1}^{N_L} U_{p_{L1}}\left[t-(l-1)\frac{T_V}{N_L}-(j-1)T_V\right], & 0 \le t \le \tau \\ 0, & \tau < t \le T \end{cases} \tag{5}$$

where N_L is the number of main rotor blades, T_V is the rotation period, J is the number of rotation cycles, $\tau = JT_V$ is the pulse width of radiated acoustic signal, T is the total signal duration, and $U_{p_{L1}}(t)$ is the acoustic pressure signal generated by a single blade during one cycle:

$$U_{p_{L1}}(t) = \begin{cases} U_{p_{L1\text{-}pr}}(t) + U_{p_{L1\text{-}ud}}(t), & 0 \le t \le T_V \\ 0, & t > T_V \end{cases} \tag{6}$$

where $U_{p_{L1\text{-}pr}}(t)$ and $U_{p_{L1\text{-}ud}}(t)$ are respectively the high-pressure and low-pressure signals generated by the rotor blade. The expressions are expressed as following:

$$U_{p_{L1\text{-}pr}}(t) = \begin{cases} 0, & 0 \le t < t_{f.s-N} \\ k_{rt} k_{p0-\alpha} \dfrac{\rho 2\pi^2 r_{sL}^2}{T_V^2}\left(1+\dfrac{k_{N-\alpha}}{R_L} r_{sL}\right), & t_{f.s-N} \le t \le t_{f.s-K} \\ 0, & t > t_{f.s-K} \end{cases} \tag{7}$$

$$U_{p_{L1\text{-}ud}}(t) = \begin{cases} 0, & 0 \le t < t_{f.s-NU} \\ -k_{rt} k_{u0-\alpha} \dfrac{\rho 2\pi^2 r_{sL}^2}{T_V^2}\left(1+\dfrac{k_{N-\alpha}}{R_L} r_{sL}\right), & t_{f.s-NU} \le t \le t_{f.s-KU} \\ 0, & t > t_{f.s-KU} \end{cases} \tag{8}$$

where k_{rt} is the acoustic attenuation coefficient from the rotor to the coupling point, k_{p0_α} is the angle of attack coefficient at the blade root, and $k_{N-\alpha}$ is the pressure variation coefficient induced by angle of attack variations along the radial blade. The parameter ρ is the undisturbed flow density, r_{sL} is the radial distance from an arbitrary point on the blade to the rotor center, and R_L is the radial distance from blade tip to rotor center (rotor disk radius). The parameters $t_{f.s-N}$ and $t_{f.s-K}$ are the initial time and the final time of the high-pressure signal respectively, and their calculation is correspondingly related with the radial distance from the blade root to the rotor center r_{sN} and the rotor disk radius R_L. The parameters of the low-pressure signal follow analogous definitions to the above, hence their descriptions are not reiterated for brevity.

The acoustic-seismic coupling accomplishes the conversion of acoustic pressure into seismic vibration source at the coupling point, it can be quantified by the coupling coefficient ε. Then the

vibration amplitude at the coupling point can be expressed as:

$$U_t(t)=\varepsilon U_{p_L}(t)=\begin{cases}\sum_{j=1}^{J}\sum_{l=1}^{N_L}\varepsilon U_{p_{L1}}\left[t-(l-1)\frac{T_V}{N_L}-(j-1)T_V\right], & 0\le t\le\tau\\ 0, & \tau<t\le T\end{cases} \tag{9}$$

where $U_t(t)$ corresponds to A_0 defined in Eq.(4). The frequency spectrum of the vibration signal obtained after discrete Fourier transform (DFT) is as follows:

$$G_t(k)=DFT\left[U_t(n)\right]=\sum_{n=0}^{N-1}U_t(n)\exp\left(-j\frac{2\pi}{N}kn\right),\ k=0,\ldots,N-1 \tag{10}$$

Frequency Response of Rayleigh Wave Attenuation. The frequency-dependent attenuation characteristics of Rayleigh waves can be formulated by frequency response as[4]:

$$G_{SR}(k,r)=\left|G_{SR}(k,r)\right|\exp\left(-j2\pi f_k\frac{r}{V_R}\right) \tag{11}$$

where the phase factor $\exp\left(-j2\pi f_k\frac{r}{V_R}\right)$ denotes the phase shift due to time delay, in which f_k represents the discrete frequency. Following Eq.(4), the amplitude-frequency response of attenuation can be explicitly expressed as:

$$\left|G_{SR}(k,r)\right|=K_P(r)D_{SR}(k,r) \tag{12}$$

In the above equation, the factors $K_P(r)=r^{-0.5}$ and $D_{SR}(k,r)=\exp\left(-\alpha_0 f_k r\right)$ correspond to geometric divergence and absorption attenuation, respectively.

Models of Signal Received by Sensor. The frequency spectrum of the signal received by the seismic sensor is:

$$G_r(k,r)=G_t(k)G_{SR}(k,r) \tag{13}$$

The seismic wave's discrete time-domain signal at the receiving point is obtained via the inverse discrete Fourier transform (IDFT) of its spectrum:

$$U_r(n,r)=IDFT\left[G_r(k,r)\right]=\frac{1}{N}\sum_{k=0}^{N-1}G_r(k,r)\exp\left(j\frac{2\pi}{N}kn\right),\ n=0,\ldots,N-1 \tag{14}$$

Numerical Simulation Experiment. The simulation parameters listed in Table 3 are established based on helicopter design specifications and aerodynamic acoustic theories, combined with research on seismic wave attenuation characteristics. Figure 10 shows the acoustic pressure signals generated by a single blade at the coupling point during one cycle: high-pressure in blue, low-pressure in black, and superimposed signal $U_{p_{L1}}(t)$ in red.

Table 3 - Simulation parameters of the helicopter main rotor

Parameter	Symbol	Value	Unit	Parameter	Symbol	Value	Unit
Number of blades	N_L	5	-	Rayleigh wave phase velocity	V_R	350	m/s
Rotational speed	N_{rpm}	192	rpm	Frequency-independent attenuation coefficient	α_0	0.50×10^{-3}	s/m
Rotation period	T_V	0.3125	s	Undisturbed flow density	ρ	1.225	kg/m^3

Distance from blade root to rotor center	r_{sN}	0.87	m	Acoustic pressure attenuation coefficient	k_{rt}	0.005	-
Distance from blade tip to rotor center	R_L	10.647	m	Acoustic-seismic coupling coefficient	ε	5×10^{-6}	(m/s)/Pa
High-pressure coefficient at blade root	k_{p0_α}	0.02	-	Number of rotation cycles	J	2	-
Low-pressure coefficient at blade root	k_{u0_α}	0.02	-	Pulse width of radiated acoustic signal	τ	0.625	s
Radial pressure variation coefficient	$k_{N-\alpha}$	0.1		Signal total duration	T	4.096	s

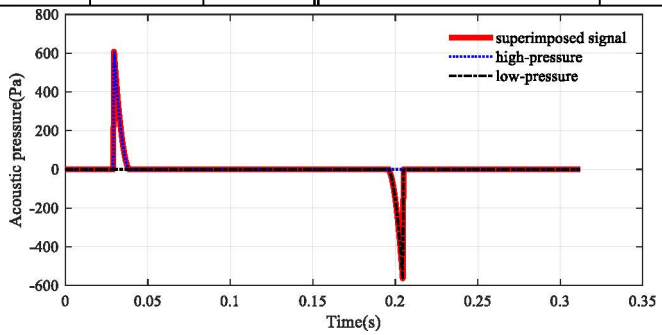

Figure 10 - The acoustic pressure signal of a single blade in a single cycle

Due to the periodic rotor motion, Figure 11(a) shows vibration waveforms with a period of approximately $T_0 = 0.0625\text{s}$. And Figure 11(b) shows discrete harmonics on the broadband noise, matching the spectrum characteristics of aerodynamic noise. The fundamental frequency $f_0 = 1/T_0 = 16\text{Hz}$ aligns with theoretical blade passing frequency (BPF) calculated as $f_{BPF} = N_L N_{rpm}/60 = 16\text{Hz}$.

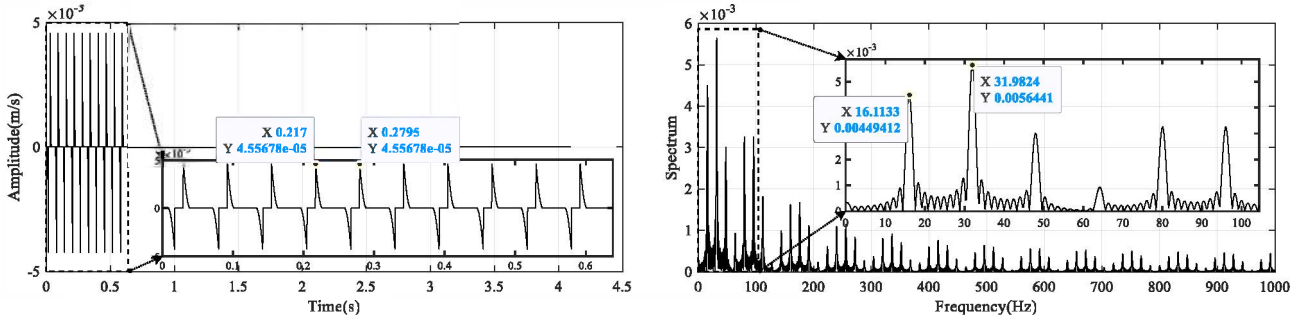

(a) (b)

Figure 11 - The vibration signal and its spectrum at the coupling point

The frequency-dependent attenuation coefficient α is presented in Figure 12. Different distances r are set to analyze the attenuation effects in Eq.(11). Then the time and frequency characteristics of the vibration signal received by the sensor at different distances r are presented in Figure 13.

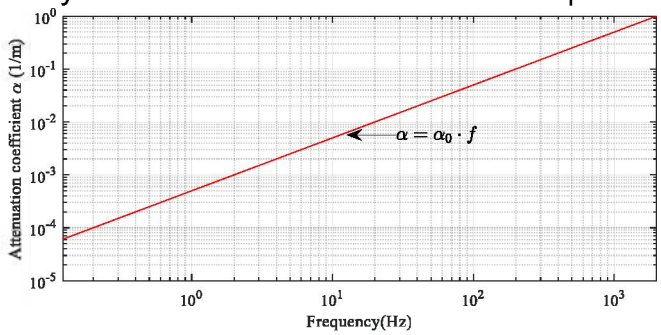

Figure 12 - The attenuation coefficient of Rayleigh waves

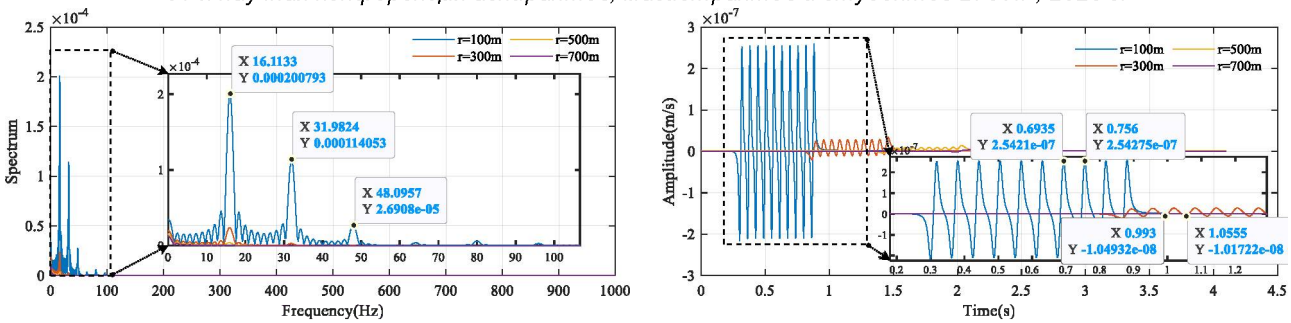

(a) (b)

Figure 13 - The vibration signal and its spectrum received by the sensor

Figure 13(a) demonstrates that the received signal spectrum exhibits discrete harmonic and bandwidth reduction. The latter results from the non-uniform frequency absorption attenuation of Rayleigh waves—weaker low-frequency attenuation and rapid high-frequency attenuation. With increasing propagation distance, the fundamental frequency f_0 and low-order harmonics gradually diminish. The spectrum further reveals an attenuation mechanism transition from dominant exponential absorption at short distances to prevailing power-law geometric divergence at long distances. Figure 13(b) displays periodic waveform with a fundamental period matching the acoustic signals in Figure 11, where progressive high-frequency suppression due to distance increase leads to bandwidth reduction, waveform smoothing, and prolonged signal duration.

Conclusion. The frequency-dependent attenuation in the ground of the helicopter main rotor acoustic pressure signals after coupling, constitutes a complex physical phenomenon, whose attenuation magnitude is predominantly governed by vibration frequency and medium properties, exerting direct effects on the signals received by sensors. This integrated modeling framework establishes theoretical foundations for helicopter detection, localization, and identification algorithms.

Reference

[1] *M. E. Goldstein,* Aeroacoustics. *New York: McGraw-Hill International Book Company, 1976.*

[2] *G. A. Athanasopoulos, P. C. Pelekis, and G. A. Anagnostopoulos, "Effect of soil stiffness in the attenuation of Rayleigh-wave motions from field measurements,"* Soil Dynamics and Earthquake Engineering, *vol. 19, no. 4, pp. 277–288, 2000,*

[3] *A. M. Jackie and A. S. Heister, "Basic physics of acoustic wave forming performed by the aircraft propeller and mathematical model of acoustic signal time structure of the ideal blade,"* Doklady BSUIR, *vol. 3, no. 33, pp. 20–26, 2008.*

[4] *S. R. Heister, R. V. Bykov, and A. M. Jackie, "The Evolution of the Temporal and Spectral Structures of the Acoustic Signal of a Shot (Explosion) as it Propagates through the Air,"* Bulletin of the Military Academy of the Republic of Belarus, *vol. 17, no. 4, pp. 67–75, 2007.*

МОДЕЛИРОВАНИЕ АТТЕНЮАЦИИ СЕЙСМИЧЕСКИХ ВОЛН ДЛЯ ОБНАРУЖЕНИЯ ВЕРТОЛЁТОВ

Лю Сяоцзюнь, Ван Чжуан

Национальный университет оборонных технологий, Чанша, Китай

Аннотация. Технология обнаружения сейсмических волн предоставляет жизнеспособное решение для мониторинга вертолётов на малых высотах в пограничном воздушном пространстве. В данной статье предлагается модель аттенюации сейсмических волн, которая проверяется с помощью численных симуляций.